

The Most Luminous Galaxies

I. Félix Mirabel^{1,2}

¹ CEA/DSM/DAPNIA, Service d'Astrophysique, 91191 Gif/Yvette. France

² IAFE/CONICET. cc 67, suc 28. Ciudad Universitaria. 1428 Buenos Aires. Argentina

Abstract. Ultraluminous galaxies in the local universe ($z \leq 0.2$) emit the bulk of their energy in the mid and far-infrared. The multiwavelength approach to these objects has shown that they are advanced mergers of gas-rich spiral galaxies. Galaxy-galaxy collisions took place on all cosmological time-scales, and nearby mergers serve as local analogs to gain insight into the physical processes that lead to the formation and transformation of galaxies in the more distant universe. Here I review multiwavelength observations –with particular emphasis on recent results obtained with ISO– of mergers of massive galaxies driving the formation of: 1) luminous infrared galaxies, 2) elliptical galaxy cores, 3) luminous dust-enshrouded extranuclear starbursts, 4) symbiotic galaxies that host AGNs, and 5) tidal dwarf galaxies. The most important implication for studies on the formation of galaxies at early cosmological timescales is that the distant analogs to the local ultraluminous infrared galaxies are invisible in the ultraviolet and optical wavelength rest-frames and should be detected as sub-millimeter sources with no optical counterparts.

1 Luminous Galaxies

One of the most important discoveries from extragalactic observations at mid- and far-infrared wavelengths has been the identification of a class of “Luminous Infrared Galaxies” (LIGs), objects that emit more energy in the infrared ($\sim 5\text{--}500\mu\text{m}$) than at all other wavelengths combined (see [18] for a comprehensive review). The first all-sky survey at far-infrared wavelengths carried out in 1983 by the *Infrared Astronomical Satellite (IRAS)* resulted in the detection of tens of thousands of galaxies, the vast majority of which were too faint to have been included in previous optical catalogs. It is now clear that part of the reason for the large number of detections is the fact that the majority of the most luminous galaxies in the Universe are extremely dusty. Previous assumptions, based primarily on optical observations, about the relative distributions of different types of luminous galaxies—e.g. starbursts, Seyferts, and quasi-stellar objects (QSOs)—need to be revised.

Galaxies bolometrically more luminous than $\sim 4L^*$ (i.e. $L_{bol} \geq 10^{11}L_\odot$) appear to be heavily obscured by dust. Although luminous infrared galaxies (hereafter LIGs: $L_{ir} > 10^{11}L_\odot$) are relatively rare objects, reasonable assumptions about the lifetime of the infrared phase suggest that a substantial fraction of all galaxies with $L_B > 10^{10}L_\odot$ pass through such a stage of intense infrared emission [23].

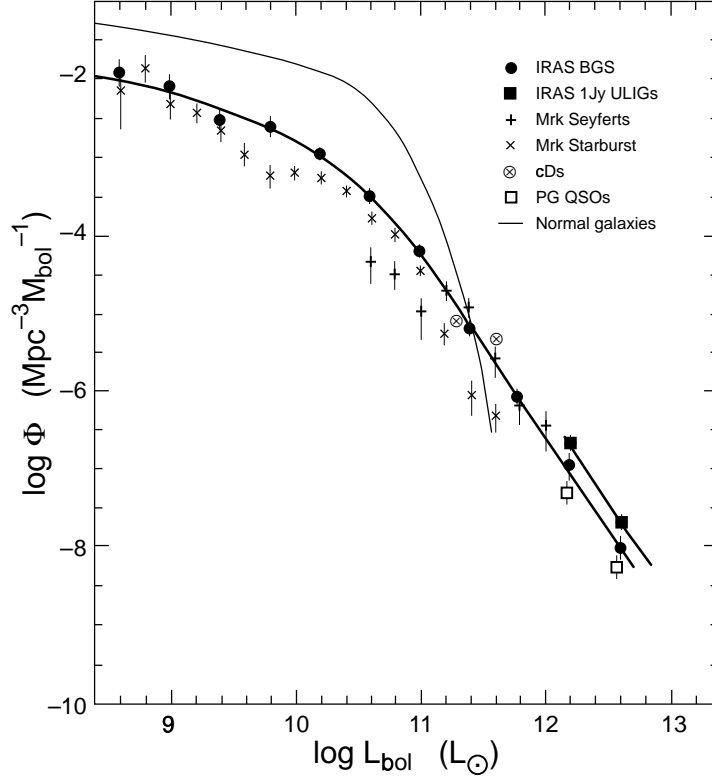


Fig. 1. Galaxy luminosity function of Infrared Galaxies compared with other extragalactic objects in the local universe. Among the most luminous galaxies ($L_{bol} > 10^{11.5} L_\odot$), infrared galaxies selected from the IRAS survey outnumber optically selected Seyferts and quasars. For references see [18].

A comparison of the luminosity function of infrared bright galaxies with other classes of extragalactic objects in the local universe is shown in Figure 1. At luminosities below $10^{11} L_\odot$, *IRAS* observations confirm that the majority of optically selected objects are relatively weak far-infrared emitters. Surveys of Markarian galaxies confirm that both Markarian starbursts and Seyferts have properties (e.g. f_{60}/f_{100} and L_{ir}/L_B ratios) closer to infrared selected samples as does the subclass of optically selected interacting galaxies. However because the most luminous galaxies are enshrouded in dust, relatively few objects in optically selected samples are found with $L_{ir} > 10^{11.5} L_\odot$.

The high luminosity tail of the infrared galaxy luminosity function is clearly in excess of what is expected from the Schechter function. For $L_{bol} = 10^{11} - 10^{12} L_\odot$, LIGs are as numerous as Markarian Seyferts and ~ 3 times more numerous than Markarian starbursts. Ultraluminous infrared galaxies (hereafter

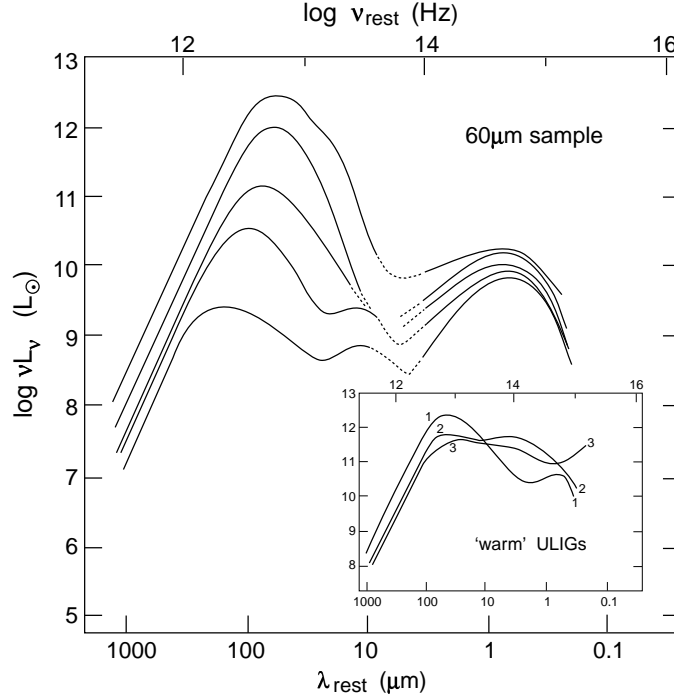


Fig. 2. Variation of the mean Spectral Energy Distribution (from submillimeter to UV wavelengths) with increasing L_{ir} for a 60 μm sample of infrared galaxies. (Insert) Examples of the subset ($\sim 15\%$) of ULIGs with “warm” infrared color ($f_{25}/f_{60} > 0.3$). Three objects (1—the powerful Wolf-Rayet galaxy IRAS 01002-2238, 2—the “infrared QSO” IRAS 07598+6508, 3—the optically selected QSO I Zw 1) are shown in the inset. For references see [18].

ULIGs: $L_{ir} > 10^{12} L_\odot$) appear to be ~ 2 times more numerous than optically selected QSOs, the only other previously known population of objects with comparable bolometric luminosities.

Although LIGs comprise the dominant population of extragalactic objects at $L_{bol} > 10^{11} L_\odot$, they are still relatively rare. For example, Figure 1 suggests that only one object with $L_{ir} > 10^{12} L_\odot$ will be found out to a redshift of ~ 0.033 , and indeed, Arp 220 ($z = 0.018$) is the only ULIG within this volume. The total infrared luminosity from LIGs in the *IRAS* Bright Galaxy Survey (BGS) is only $\sim 6\%$ of the infrared emission in the local Universe [24].

There are preliminary indications that ULIGs have been more numerous in the past. Comparison of the space density of nearby ULIGs with the more distant population provides evidence for possible strong evolution in the luminosity function at the highest infrared luminosities. Assuming pure density evolution of

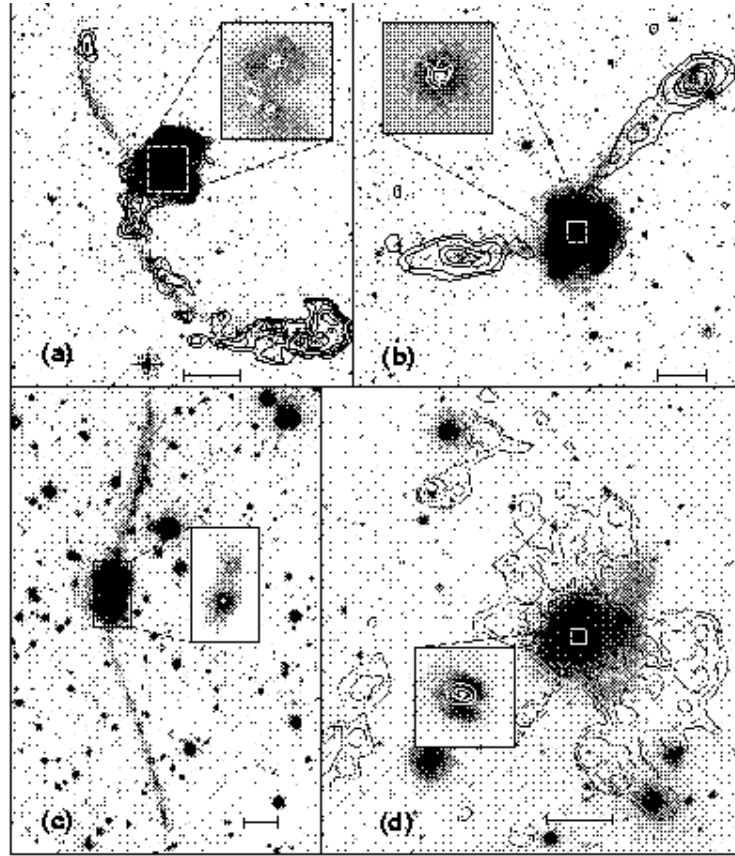


Fig. 3. Well-studied mergers: (a) NGC 4038/39 (Arp 244 = “The Antennae”); (b) NGC 7252 (Arp 226 = “Atoms for Peace”); (c) IRAS 19254–7245 (“The Super Antennae”); (d) IC 4553/54 (Arp 220). The two at the top are LIGs whereas the two at the bottom are ULIGs. Contours of H I 21-cm line column density (black) are superimposed on deep optical (*r*-band) images. Inserts show a more detailed view in the *K*-band ($2.2\mu\text{m}$) of the nuclear regions of NGC 4038/39, NGC 7252, and IRAS 19254–7245, and in the *r*-band ($0.65\mu\text{m}$) of Arp 220. White contours represent the CO($1\rightarrow 0$) line integrated intensity as measured by the OVRO millimeter-wave interferometer. No H I or CO interferometer data are available for the southern hemisphere object IRAS 19254–7245. The scale bar represents 10 kpc.

the form $\Phi(z) \propto (1+z)^n$, [8] found $n \sim 7 \pm 3$ for a complete flux-limited sample of ULIGs.

The infrared properties for the complete *IRAS* Bright Galaxy Sample have been summarized and combined with optical data to determine the relative luminosity output from galaxies in the local Universe at wavelengths $\sim 0.1\text{--}1000\mu\text{m}$ [24]. Figure 2 illustrates how the shape of the mean spectral energy distribution (SED) varies for galaxies with increasing total infrared luminosity. Systematic

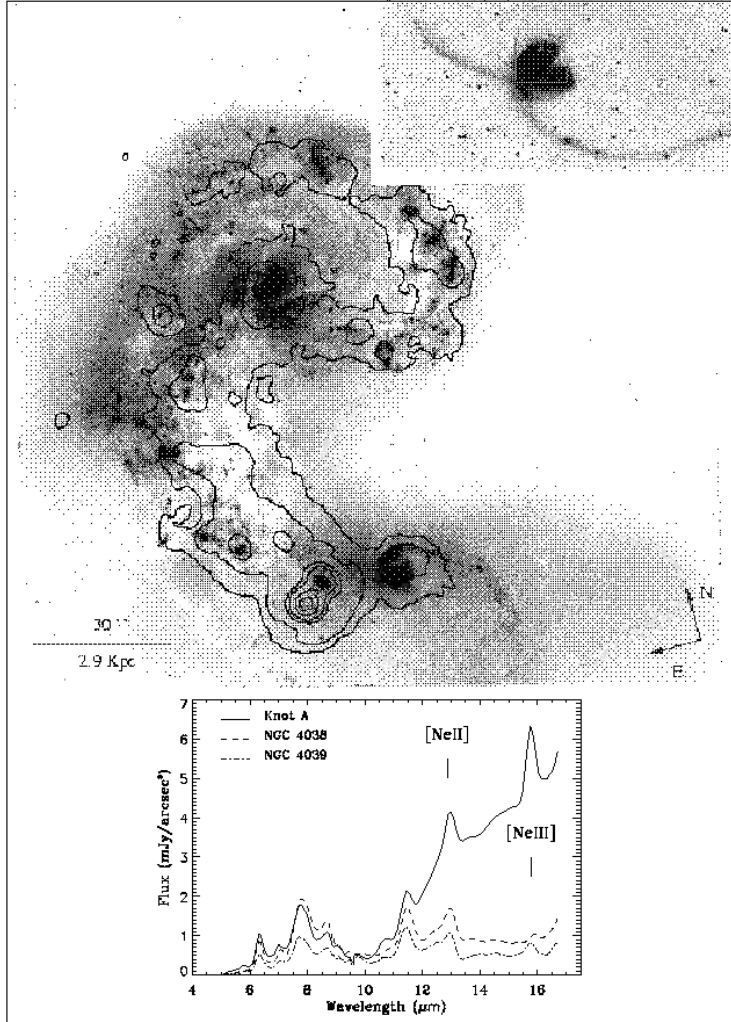


Fig.4. The upper figure from [16] shows a superposition of the mid-infrared (12 - 17 μ , contours) image of the Antennae galaxies obtained with the Infrared Space Observatory, on the composite optical image with V (5252 Å) and I (8269 Å) filters recovered from the Hubble Space Telescope archive . About half of the mid-infrared emission from the gas and dust that is being heated by recently formed massive stars comes from an off-nuclear region that is clearly displaced from the most prominent dark lanes seen in the optical. The brightest mid-infrared emission comes from a region that is relatively inconspicuous at optical wavelengths. The ISOCAM image was made with a 1.5'' pixel field of view. Contours are 0.4, 1, 3, 5, 10, and 15 mJy. The lower figure shows the spectrum of the brightest mid-infrared knot and of the nuclei of NGC 4038 and NGC 4039. The rise of the continuum above 10 μ m and strong NeIII line emission observed in the brightest mid-infrared knot indicate that the most massive stars in this system of interacting galaxies are being formed in that optically obscured region, still enshrouded in large quantities of gas and dust.

variations are observed in the mean infrared colors; the ratio f_{60}/f_{100} increases while f_{12}/f_{25} decreases with increasing infrared luminosity. Figure 2 also illustrates that the observed range of over 3 orders of magnitude in L_{ir} for infrared-selected galaxies is accompanied by less than a factor of 3–4 change in the optical luminosity.

[20] showed that a small but significant fraction of ULIGs, those with “warm” ($f_{25}/f_{60} > 0.3$) infrared colors, have SEDs with mid-infrared emission ($\sim 5\text{--}40\,\mu\text{m}$) over an order of magnitude stronger than the larger fraction of “cooler” ULIGs. These warm galaxies (Figure 2 insert), which appear to span a wide range of classes of extragalactic objects including powerful radio galaxies (PRGs: $L_{408MHz} \geq 10^{25}W\text{Hz}^{-1}$) and optically selected QSOs, have been used as evidence for an evolutionary connection between ULIGs and QSOs (e.g. [19,20]).

There is a strong correlation between the broad band colors (from optical to far-infrared) and morphological type [18]. In particular, the fraction of objects that are interacting/merger systems appears to increase systematically with increasing infrared luminosity. The imaging surveys of objects in the local universe [19,12] have shown that the fraction of strongly interacting/merger systems increases from $\sim 10\%$ at $\log(L_{ir}/L_\odot) = 10.5\text{--}11$ to $\sim 100\%$ at $\log(L_{ir}/L_\odot) > 12$. In panel (c) of Figure 3 is shown the “Super-antennae”, which is the prototype of ULIG [14]. ISO observations [10] have shown that more than 98% of the mid-infrared flux from this object comes from the southern component which hosts a Seyfert 2 nucleus.

From the detailed studies of nearby ultraluminous infrared galaxies the following conclusions were reached. 1) They are mergers of evolved gas-rich giant spiral galaxies (e.g. Milky Way with Andromeda), and not “primordial” galaxies. 2) To boost the luminosity above $10^{12} L_\odot$ the nuclei must have approached at least 10 kpc, namely, they are advanced mergers. 3) Due to the gravitational impact the interstellar gas decouples from the stars and large amounts of interstellar matter fall at high rates to the central region. This is the condition to produce a nuclear starburst, and/or feed a supermassive black hole at super-Eddington accretion rates. To produce such large accretion rates, the gravitational potential wheels of massive bulges are needed.

A workshop on the question concerning the ultimate source of energy (starbursts versus AGN’s) took place in Ringberg on October 1998. Below $2 \cdot 10^{12} L_\odot$ starbursts dominate the energy budget, but above $3 \cdot 10^{12} L_\odot$ AGN’s seem to be always present and become an important source of energy. In this respect it is interesting to note that it is found with ISO that in the prototype Seyfert 2 galaxy NGC 1068, about 80% of the mid-infrared flux between 4 and $18\,\mu\text{m}$ comes from the AGN [11].

A caveat for the subject of this conference is that the pre-encounter objects that merged at high redshifts must have been different from the metal-rich evolved galaxies merging at present. Another caveat is that ultraluminous IR galaxies at high redshifts may be very difficult to detect using the Lyman break technique. Due to the large amounts of dust in ultraluminous objects, very little or none continuum leaks out at ultraviolet wavelengths. Therefore, surveys with

submillimeter arrays as ALMA will be needed to detect ultraluminous galaxies at high redshifts.

2 ISO Observation of Extranuclear Starbursts

The starbursts in ultraluminous galaxies take place in the nuclear region. One of the new findings with ISO is a class of very luminous dust-enshrouded extranuclear starbursts in nearby spiral-spiral mergers. When the pre-encounter galaxies do not have prominent bulges, namely, when the mergers are -for instance- two Sc galaxies, the most luminous starbursts may take place in extranuclear regions that are inconspicuous at optical wavelengths. These extranuclear starbursts have sizes ≤ 100 pc in radius and can produce up to 50% of the overall mid-infrared output from these systems. Furthermore, the analyses of the mid-infrared spectra indicate that the most massive stars in these systems are formed inside these optically invisible knots.

In Figure 4 is shown in contours the mid-infrared (12-17 μm) image of the Antennae galaxies obtained with ISO [16], superimposed on the optical image from HST. Below are shown representative spectra of the two nuclei and the brightest mid-infrared knot. It shows that the most massive stars are formed in an obscured knot of 50 pc radius, which produces about 15% of the total luminosity from the Antennae galaxies between 12.5 and 17 μm . A more extreme case is found in NGC 3690 [6], where it is observed an extranuclear region ≤ 100 pc in radius that radiates $\sim 45\%$ of the overall mid-infrared output from this system. If the fraction of far-infrared fluxes is the same as in the mid-infrared, such compact region produces a luminosity of $2 \cdot 10^{11} L_\odot$. Therefore, the luminosity of a few compact starburst knots of this type would be comparable to the total bolometric luminosity of a ULIG such as Arp 220 (Figure 3d).

The multiwavelength view of this nearby sample of prototype merging systems suggests caution in deriving scenarios of early evolution of galaxies at high redshift using only observations in the narrow rest-frame ultraviolet wavelength range [16]. Although the actual numbers of this type of systems may not be large, we must keep in mind that the most intense starbursts are enshrouded in dust and no ultraviolet light leaks out from these regions.

3 Symbiotic Galaxies

Giant radio galaxies are thought to be massive ellipticals powered by accretion of interstellar matter onto a supermassive black hole. Interactions with gas rich galaxies may provide the interstellar matter to feed the active galactic nucleus (AGN). To power radio lobes that extend up to distances of hundreds of kiloparsecs, gas has to be funneled from kiloparsec size scales down to the AGN at rates of $\sim 1 M_\odot \text{ yr}^{-1}$ during $\geq 10^8$ years. Therefore, large and massive quasi-stable structures of gas and dust should exist in the deep interior of the giant elliptical hosts of double lobe radio galaxies. Recent mid-infrared observations

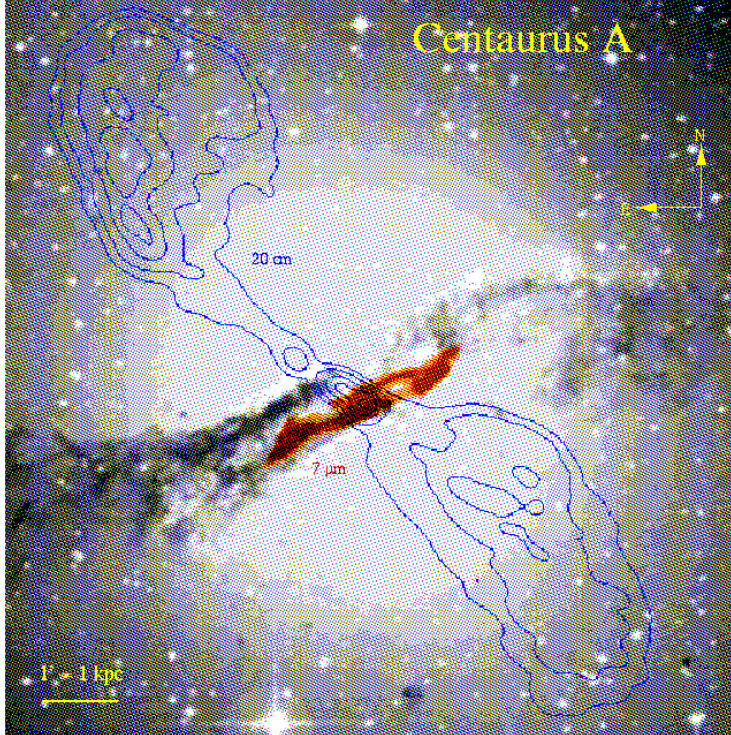


Fig. 5. The ISO $7\text{ }\mu\text{m}$ emission (dark structure; [17]) and VLA 20 cm continuum in contours [1], overlaid on an optical image from the Palomar Digital Sky Survey. The emission from dust with a bisymmetric morphology at the centre is about 10 times smaller than the overall size of the shell structure in the elliptical and lies on a plane that is almost parallel to the minor axis of its giant host. Whereas the gas associated to the spiral rotates with a maximum radial velocity of 250 km s^{-1} , the ellipsoidal stellar component rotates slowly approximately perpendicular to the dust lane [27]. The synchrotron radio jets shown in this figure correspond to the inner structure of a double lobe radio source that extends up to 5° ($\sim 300\text{ kpc}$) on the sky. The jets are believed to be powered by a massive black hole located at the common dynamic center of the elliptical and spiral structures.

with ISO revealed for the first time a bisymmetric spiral structure with the dimensions of a small galaxy at the centre of Centaurus A [17]. The spiral was formed out of the tidal debris of accreted gas-rich object(s) and has a dust morphology that is remarkably similar to that found in barred spiral galaxies (see Figure 5). The observations of the closest AGN to Earth suggest that the dusty hosts of giant radio galaxies like CenA, are “symbiotic” galaxies composed of a barred spiral inside an elliptical, where the bar serves to funnel gas toward the AGN.

The barred spiral at the centre of CenA has dimensions comparable to that of the small Local Group galaxy Messier 33. It lies on a plane that is almost parallel to the minor axis of the giant elliptical. Whereas the spiral rotates with maximum radial velocities of $\sim 250 \text{ km s}^{-1}$, the ellipsoidal stellar component seems to rotate slowly (maximum line-of-sight velocity is $\sim 40 \text{ km s}^{-1}$) approximately perpendicular to the dust lane. The genesis, morphology, and dynamics of the spiral formed at the centre of CenA are determined by the gravitational potential of the elliptical, much as a usual spiral with its dark matter halo. On the other hand, the AGN that powers the radio jets is fed by gas funneled to the center via the bar structure of the spiral. The spatial co-existence and intimate association between these two distinct and dissimilar systems suggest that Cen A is the result from a cosmic symbiosis.

4 Formation of Ellipticals

In disk-disk collisions of galaxies, dynamical friction and subsequent relaxation may produce a mass distribution similar to that in classic elliptical galaxies. From the relative numbers of mergers and ellipticals in the New General Catalogue [26] estimated that a large fraction of ellipticals could be formed via merging. The first direct observational evidence for the transition from a disk-disk merger toward an elliptical was presented in the optical study of NGC 7252 by [22]. The brightness distribution over most of the main body of this galaxy which is shown in Figure 3c is closely approximated by a de Vaucouleurs ($r^{-1/4}$) profile. However, NGC 7252 still contains large amounts of interstellar gas and exhibits a pair of prominent tidal tails (see Figure 3b); neither property is typical of ellipticals.

Near-infrared images are less affected by dust extinction and also provide a better probe of the older stellar population, which contains most of the disk mass and therefore determines the gravitational potential. *K*-band images of six mergers by [28] showed that the infrared radial brightness profiles for two LIGs—Arp 220 and NGC 2623—follow an $r^{-1/4}$ law over most of the observable disks. Among eight merger remnants, [25] found *K*-band brightness profiles for four objects that were well fitted by an $r^{-1/4}$ law over most of the observable disks. [8] finds a similar proportion ($\sim 50\%$) of ULIGs whose *K*-band profiles are well fit by a $r^{-1/4}$ law.

More recently, [9] have proposed that ULIGs are elliptical galaxies forming by merger-induced dissipative collapse. The extremely large central gas densities ($\sim 10^2\text{--}10^3 M_\odot \text{ pc}^{-3}$) observed in many nearby ULIGs, and the large stellar velocity dispersions found in the nuclei of Arp 220 and NGC 6240 are comparable to the stellar densities and velocity dispersions respectively, in the central compact cores of ellipticals.

Despite the *K*-band and CO evidence that LIGs may be forming ellipticals, we still need to account for two important additional properties of ellipticals: 1. the large population of globular clusters in the extended halos of elliptical galaxies, which cannot be accounted for by the sum of globulars in two preexisting spirals, and 2. the need to remove the large amounts of cold gas and

dust present in infrared-luminous mergers in order to approximate the relative gas-poor properties of ellipticals. These two issues have been discussed by [18].

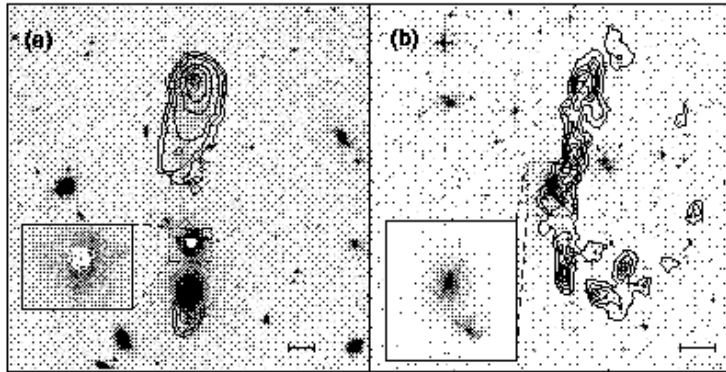


Fig. 6. (a) *NGC 3561A/B (Arp 105)* from [3]; (b) *NGC 5291A/B ("Sea shell")* from [4]. Tidal dwarfs may have different morphologies: Blue compacts, Magellanic Irregulars, and Dwarf Irregulars. Contours of HI 21-cm line column density (black) are superimposed on deep optical (*r*-band) images. Inserts show a more detailed view in *r*-band of the spiral galaxy NGC 3561A [3], and of the interacting pair NGC 5291A/B. White contours represent the CO(1→0) line integrated intensity as measured by the IRAM millimeter-wave interferometer. CO emission has not been detected in NGC 5291A/B. The scale bar represents 20 kpc.

5 Tidal Dwarf Galaxies

Collisions between giant disk galaxies may trigger the formation of dwarf galaxies. This idea, which was first proposed by [29] and later by [21], has received recent observational support [14, 15, 5, 3]. Renewed interest in this phenomenon arose from the inspection of the optical images of ULIGs, which frequently exhibit patches of optically emitting material along the tidal tails (see Figure 3a–c). These objects appear to become bluer near the tips of the tails at the position of massive clouds of HI. These condensations have a wide range of absolute magnitudes, $M_V \sim -14$ to -19.2 , and HI masses, $M(HI) \sim 5 \times 10^8$ to $6 \times 10^9 M_\odot$. [13] have shown that objects resembling irregular dwarfs, blue compacts, and irregulars of Magellanic type are formed in the tails. These small galaxies of tidal origin are likely to become detached systems, namely, isolated dwarf galaxies. Because the matter out of which they are formed has been removed from the outer parts of giant disk galaxies, the tidal dwarfs we observe forming today have a metallicity of about one third solar [2].

It is interesting that in these recycled galaxies of tidal origin there is—as in globular clusters—no compelling evidence for dark matter [13]. To find the true

fraction of dwarf galaxies that may have been formed by processes similar to the tidal interactions we observe today between giant spiral galaxies, more extensive observations of interacting systems will be needed. A recent step forward is the statistical finding that perhaps as much as one half of the dwarf population in groups is the product of interactions among the parent galaxies [7].

Tidal dwarfs are formed not only during spiral-spiral mergers, but also in encounters of spirals with massive ellipticals in clusters of galaxies. In Figure 6 are shown the results from the multiwavelength study of Arp 105 and NGC 5291A/B which are in clusters of galaxies. In Arp 105, [3] find tidal dwarfs that resemble Magellanic Irregulars and a blue compact. In NGC 5291, about 10 tidal dwarfs of irregular morphology are found associated to the 200 kpc HI ring shown in Figure 6 [4].

6 Conclusions

- 1) Scenarios on the history of star formation that use only observations in the UV and optical rest-frames result in luminosity functions that are strongly biased in the high luminosity end.
- 2) The most luminous nuclear and off-nuclear starbursts are enshrouded in dust. In merging galaxies ISO revealed off-nuclear starburst knots with sizes ≤ 100 pc that produce bolometric luminosities of up to $2 \cdot 10^{11} L_\odot$ (e.g. NGC 3690). A few of these starburst knots can produce the overall bolometric luminosity of an ultraluminous galaxy such as Arp 220.
- 3) The observation with ISO of the nearest AGN to Earth (Centaurus A) opens the general question on whether the hosts of giant radio galaxies are symbiotic galaxies composed of spirals at the centre of giant ellipticals.
- 4) Mergers of disks can produce metal-rich elliptical galaxy cores.
- 5) Collisions between giant disk galaxies trigger the formation of dwarf galaxies out tidal debris. A fraction of these re-cycled galaxies become detached systems with diverse morphologies: blue compact dwarfs, dwarf irregulars, and irregulars of Magellanic type.

Acknowledgements: Most of the work review here was carried out in collaboration with D.B. Sanders, P-A. Duc, V. Charmandaris and O. Laurent.

References

1. J.J. Condon et al.: A&ASS **103**, 81 (1996)
2. P.-A. Duc: Genèse de galaxies naines dans les systèmes en interaction. PhD thesis, Univ. Paris (1995)
3. P.-A. Duc & I. F. Mirabel: A&A **289**, 83 (1994)
4. P.-A. Duc & I. F. Mirabel: A&A **333**, 813 (1998)
5. B. G. Elmegreen, M. Kaufman, M. Thomasson: ApJ **412**, 90 (1993)
6. P. Gallais et al.: The Universe as seen by ISO, ESA/SP-427 vol. 2, 881 (1999)
7. S. D. Hunsberger, J. C. Charlton, D. Zaritsky: ApJ **462**, 50 (1996)

8. D. C. Kim: The IRAS 1 Jy survey of ultraluminous infrared galaxies. PhD thesis, Univ. Hawaii (1995)
9. J. Kormendy, D. B. Sanders: ApJ **390**, L53 (1992)
10. O. Laurent, V. Charmandaris, I. F. Mirabel et al.: A&A **359**, 359 (2000)
11. E. Le Floc'h, I. F. Mirabel, O. Laurent et al.: A&A **367**, 487 (2001)
12. J. Melnick, I. F. Mirabel: A&A **231**, L19 (1990)
13. I. F. Mirabel, P.-A. Duc, H. Dottori: In *Dwarf Galaxies*, ed. G Meylan, P Prugniel, p. 371. Garching bei Munchen:ESO (1995)
14. I. F. Mirabel, D. Lutz, J. Maza: A&A **243**, 367 (1991)
15. I. F. Mirabel, H. Dottori, D. Lutz: A&A **256**, L19 (1992)
16. I. F. Mirabel, L. Vigroux, V. Charmandaris et al.: A&A **333**, L1 (1998)
17. I. F. Mirabel, O. Laurent, D. B. Sanders et al.: A&A **341**, 667 (1999)
18. D. B. Sanders, I. F. Mirabel: ARAA **34**, 749 (1996)
19. D. B. Sanders, B. T. Soifer, J. H. Elias, et al.: ApJ **325**, 74 (1998)
20. D. B. Sanders, B. T. Soifer, J. H. Elias, G. Neugebauer, K. Matthews: ApJ **328**, L35 (1998)
21. F. Schweizer: In *Structure and Properties of Nearby Galaxies*, ed. EM Berkhuijsen, R Wielebinski, p. 279. Dordrecht:Reidel (1978)
22. F. Schweizer: ApJ **252**, 455 (1982)
23. B. T. Soifer, D. B. Sanders, B. F. Madore, G. Neugebauer, et al.: ApJ **320**, 238 (1987)
24. B. T. Soifer, G. Neugebauer: AJ **101**, 354 (1991)
25. S. A. Stanford, H. A. Bushouse: ApJ **371**, 92 (1991)
26. A. Toomre: In *The Evolution of Galaxies and Stellar Populations*, ed. BM Tinsley, RB Larson, p. 401. New Haven, CT:Yale Univ. Obs. (1977)
27. A. Wilkinson et al.: MNRAS **218**, 297 (1986)
28. G. S. Wright, P. A. James, R. D. Joseph, I. S. McLean: Nature **344**, 417 (1990)
29. F. Zwicky: Ergeb. Exakten Naturwiss. **29**, 34 (1956)